RSC Advances

PAPER

View Article Online
View Journal | View Issue

Cite this: *RSC Adv.*, 2025, **15**, 20935

An efficient pathway to high persistence length helicenes from scalable [4]-helicene synthons†

Garrett L. Reinhard, *[a] Reed Dowling,[ac] Patrick Hewitt, [ab] Vikas Varshney [a] and Davide L. Simone *[a]

Received 16th April 2025
Accepted 10th June 2025

DOI: 10.1039/d5ra02685g

rsc.li/rsc-advances

A convergent synthetic strategy to high-persistence length helicenes *via* a regioselective and scalable menthyloxycarbonato-[4]-helicene synthon accessed in 84% yield is reported. To demonstrate the utility of the [4]-helicene building block, bis(menthyloxycarbonato)-[11]-helicene diastereomers were prepared *via* palladium-mediated cross-couplings, followed by a Mallory-type photo-induced annulation reaction. Our synthetic strategy leverages Stille and Heck couplings to synthesize bis(aryl)ethene precursors that exhibit preferential formation of helical products *via* 6π-electrocyclization. [11]-Helicene product yields are enhanced from 7 to 42% by maintaining photoreaction temperatures above 40 °C limiting linear and cyclobutane byproduct formation while recrystallization yielded diastereo-enrichment. This work enables the end goal of embedding enantiopure hydroxy-terminated helicenes into polymer backbones to create chiroptical responsive strain sensors.

Introduction

Helicenes are a class of *ortho*-fused aromatic rings that are inherently chiral, existing as a right- and left-handed helix, notated as *P* and *M* respectively. Though they have no chiral centers, helicenes have a C_2-axis of symmetry that exists perpendicular to the helical axis, making the molecule chiral.[1] Conformational distortion of the helicene, resulting from intramolecular steric repulsions, grows greater as the length of the helicene increases, meaning that larger helicenes have an ever exaggerated helical pitch and as a result, enhanced optical properties.[2] Due to their inherent aromaticity, helicity, and large optical dichroism, they provide unique molecular and macromolecular architectures that enable the formation of dichroic fibers,[3,4] molecular machines,[5,6] and high performance polymers.[7–9] Furthermore, helicenes and their derivatives are often found to be useful as chiral ligands in numerous enantioselective syntheses.[10–12] Most interestingly, due to their unique geometry, helicenes have been postulated to have properties akin to molecular springs.[13–15]

Our interests lie in exploring the viability of helicenes as sensors and their potential to racemize under the application of a mechanical force or temperature change while bonded within a polymer backbone. To that end, we wish to develop a versatile synthesis of end-terminal functional helicenes, whereupon inversion barriers can be tailored as a function of helicene length.[14] Before embarking on developing a highly efficient synthesis of helicenes, we feel it important to review various synthetic methodologies that have been reported in the literature particularly toward the isolation of optically active (non-racemic) helicenes.

The synthesis of carbohelicenes follow five main mechanistic routes; the photocyclization, the Diels–Alder reaction, Friedel–Crafts-type reactions, metal catalyzed cyclizations, and radical cyclizations.[1] The synthetic pathway focused upon in this work is the Mallory reaction, a photochemical–electrocyclization–elimination type reaction developed by Mallory *et al.* in which stilbenes are subjected to ultraviolet radiation forming dihydro-intermediates which subsequently undergo an (dihydro) elimination reaction in the presence of an oxidant, commonly a catalytic amount of elemental iodine.[16] This synthesis was improved upon by Katz *et al.*, in which a stoichiometric amount of iodine is used in the presence of propylene oxide in an air free environment.[17] Of the synthetic mechanisms reviewed, the Katz photocyclization has been shown to have improved yields, limit the distribution of potential side products, all while needing much less intense conditions compared to the other common synthetic mechanisms.[17] It is important to note that although metal-catalyzed cyclizations tend to provide an elegant way to selectively cyclize helicene precursors, the syntheses tend to require a large number of synthetic steps.[18,19] To date, the longest helicene synthesized is a [16]-helicene that contains terminal triisopropylsilyl ether functionality, with an overall yield of less than

[a]*Air Force Research Laboratory, Polymer Branch (AFRL/RXNP), Wright-Patterson AFB, OH 45433-7750, USA. E-mail: davide.simone@us.af.mil; garrett.reinhard@us.af.mil*
[b]*AeroVironment, Inc., Dayton, OH 45432, USA*
[c]*University of Dayton, Dayton, OH 45469, USA*

† Electronic supplementary information (ESI) available: ^{1}H and ^{13}C NMR of compounds **1–7** along with crystal structures and parameters of **1–3** and **5**. CCDC 2428292–2428297. For ESI and crystallographic data in CIF or other electronic format see DOI: **https://doi.org/10.1039/d5ra02685g**

7%.[20] The goal of this publication is to define a more efficient synthetic path to high persistence length helicenes derived from [4]-helicene building blocks.

The mechanism of the Mallory-type reaction is shown in Fig. 1, where a bis(aryl)ethene undergoes photo-induced ring closure to form either a [4]-helicene or its linear analogue. Bis(aryl)ethenes are conventionally referred *via* [*x*] + [*y*] terminology, such that *x* and *y* are the number of aromatic rings bridged by an alkene. As an example, Scheme 1 showcases a [2] + [1] precursor electrocyclizing to a [4]-helicene.[21,22]

During photocyclization, in addition to expected helical and linear products, there also exists the occurrence of an intermolecular [2 + 2] cycloaddition reaction, which yields cyclobutane based side products. The side products have a greater tendency of forming when the concentration of helicene precursor is sufficiently high to enable the bi-molecular photocylization to occur. It has been reported that the formation of these side products is minimized by limiting the concentration of bis(aryl)ethene species to 1 mM for each site undergoing photocyclization.[23] This concentration limitation poses a challenge in scalable, high-yielding syntheses of helicenes, as chemists are then limited by the volume and efficiency of their photo-reaction vessel.

Developing a synthetic pathway to enable pure isolation of higher order enantiopure helicenes is highly desired for two reasons; (a) higher order helicenes possess enhanced chiroptical properties, and (b) it significantly minimizes their tendency to racemize due to a high inversion activation energy. Towards achieving this, we find that the design of the stilbene precursor has been shown to heavily influence the production of the helicene over their linear isomers.[22] The precursors that take on the design of [4] + [1] or [4] + [1] + [4] give the highest yields of un-substituted [6]- and [11]-helicene, achieving 87% and 84% isolated yields respectively. Other precursor designs, such as a [1] + [2] + [1] result in a diminished yield of [6]-helical product at 60% yield, and in some other cases, such as the [3] + [2], the linear analogue is preferred.[22]

In this work, we synthesize [2] + [1] and [4] + [1] + [4] helicene precursors to allow us to efficiently isolate [4]-helicene and [11]-helicene diastereomers enables separation into enantiopure forms. The [4]-helicene that we are reporting is terminated with a bromine to enable the synthesis of other higher order helicenes, such as a [9]- *via* a [4] + [4], a [6]- *via* a [4] + [1] or the [11]-helicene *via* [4] + [1] + [4], *etc.*

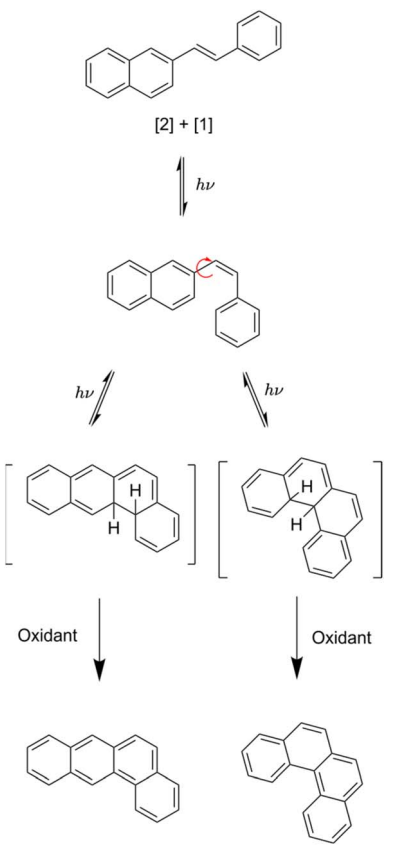

Fig. 1 Mallory cyclization reaction.

Discussion

Our synthetic strategy relies upon the use of chiral functionality appended to the helicene precursor to enhance diastereoseparation, and ultimately *P* or *M* enantiomer isolation. The use of chiral LC is also envisioned to allow for an analytically pure sample of diastereomer to be isolated to help seed single diastereomer crystallization. For the purposes of this work we have chosen the former method to report with the latter method used as a means to separate larger quantities of diastereomers. The chiral functionality also plays a role in maintaining solubility of the highly aromatic (planar) helicene precursors and is not meant to induce an enantioselective photocyclization as the functionality is too far removed from the photocyclization bond forming reaction.

(1*R*)-(+)-Menthyl chloroformate was selected as the chiral resolving agent to terminate the ends of the [11]-helicene and its precursors, enhancing solubility, enabling diastereomeric separation, and, upon removal, afford hydroxyl terminated helicenes that can be functionalized further to incorporate into polymer backbones. The first step to creating a [4] + [1] + [4] helicene precursor which is envisioned to provide improved long helicene yields, is through the efficient synthesis of a functional [4]-helicene building block, Scheme 1. Using commercially available 6-bromo-2-naphthol, (1*R*)-(+)-menthyl chloroformate was installed *via* a deprotonation of the hydroxyl group with triethylamine affording the (1*R*)-(+)-menthyl carbonate in high yielding, multi-decagram quantity batches.

Extension of the menthyl protected bromonapthyl building block to the [2] + [1] helicene precursor is achieved *via* subsequent palladium-catalyzed cross-coupling reactions, a Stille coupling followed by a chemoselective Heck coupling. The Stille couplings executed in this paper are modeled after syntheses found in the review by Farina.[24] The Heck coupling conditions were modeled after improvements made by the Buchwald group.[25]

The synthesis of **2** made use of the Farina reaction conditions without major changes. Aqueous KF washes were avoided

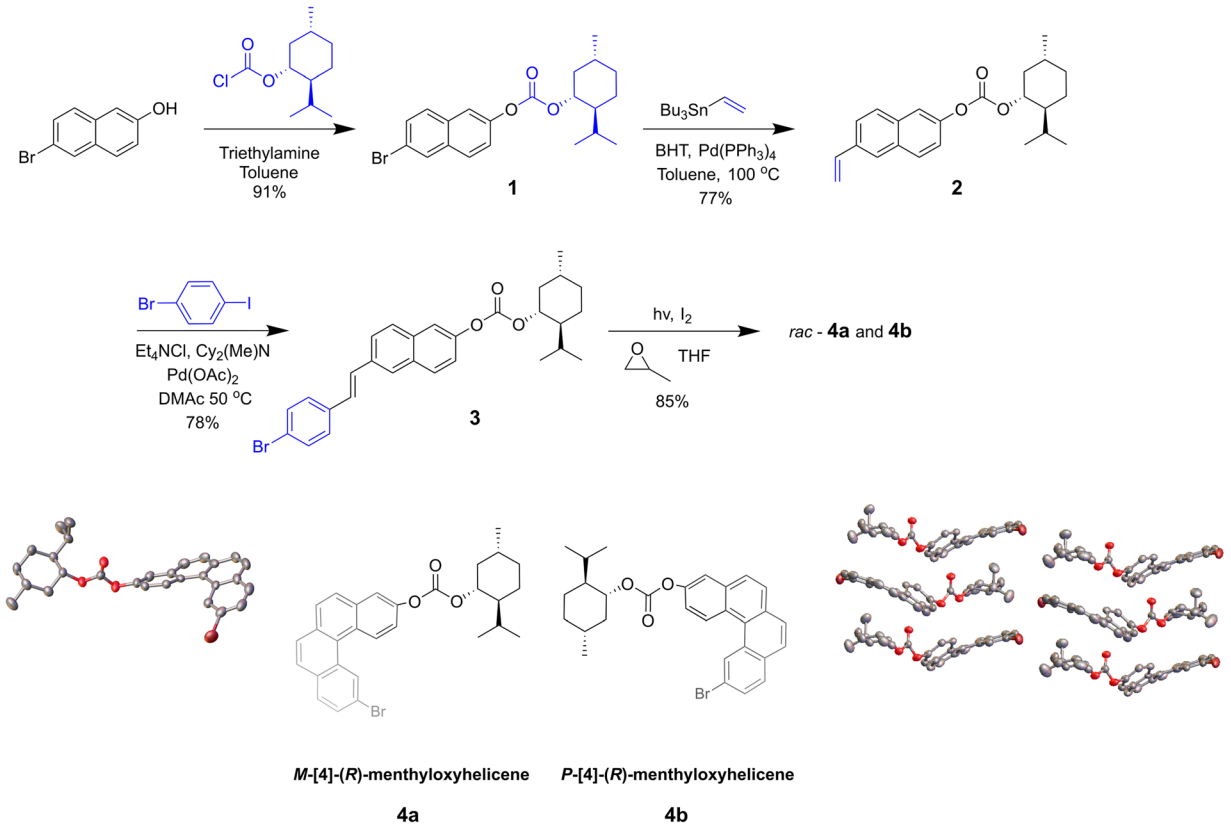

Scheme 1 Synthesis of *rac*-[4]-menthyloxycarbonato-helicene accompanied by crystal structure (left) and its packing (right). Racemic mixture is labeled from the standpoint of *P* and *M*-[4]-helicene, ignoring stereochemistry of the menthyloxycarbonato group. Butylated hydroxytoluene is abbreviated as BHT.

to reduce any risk of interaction between fluoride anions and the menthyl carbonate groups due to their susceptibility towards even mild nucleophiles. Instead, once the crude reaction mixtures were deposited onto a silica column, approximately 1–1.5 column volumes of pure hexanes was flushed through the crude material and stationary phase to remove most organotin impurities before switching to the main eluent. Further recrystallization after chromatography was required to remove residual organotin impurities in order to mitigate any potential side reactions in subsequent palladium-mediated cross couplings.

The Heck coupling of **2** with 1-bromo-4-iodobenzene was found to be chemo-selective at 50 °C, preferentially reacting with the iodo- instead of bromo-position owing to the greater ease of oxidative addition towards the weaker Ph–I bond. Reactions conducted below 50 °C yielded poor reaction progression, while increasing the temperature to 100 °C causes coupling at both halogenated positions and a total loss of chemo-selectivity.

As introduced previously, high concentrations of bis(aryl) ethenes in solution are to be avoided to reduce [2 + 2] cyclo-additions, so to improve scalability and mitigate these side products, a syringe pump (pseudo-high dilution) was utilized to add a stock solution of precursor **3** and iodine in THF at a rate in which reaction concentration was calculated to be at a constant 1 mM. Initial studies indicated *via* NMR that the cyclization of **3** to **4** fully converted within 2 hours, and so the rate of addition of precursor **3** was adjusted to match this conversion. The syringe pump method allowed for a substantial increase in scale, allowing for multi-gram quantities to be made in a single batch, as well as minimizing the potential of [2 + 2] side reactions. Without a syringe pump, using a 1 L photoreaction vessel limits scale of this reaction to yield 380 mg; with the syringe pump, an order of magnitude greater yields were achieved.

With compound **4** in hand, the synthesis of higher order helicenes is enabled, Scheme 2.

Following a similar Stille and this case a non-chemoselective Heck reaction sequence, **4** is converted to [4] + [1] + [4] helicene precursor **6** in a respectable yield. The photocyclization of **6** to the desired helicene product introduced several competing factors from a reaction optimization perspective. First, the photocyclization of **6** was designed at a 0.5 mM overall concentration, accounting for the two sites of conversion and to reduce the probability of [2 + 2] cyclo-additions. Temperature and time were two other variables that had a noticeable impact on the outcome of the reaction. Literature precedence indicates that lower temperatures favor the kinetic product (helicene) rather than the non-strained thermodynamic product (linear/pseudo-helical). During our initial attempts to photocyclize the [4] + [1] + [4], the photo-reaction vessel was chilled with an

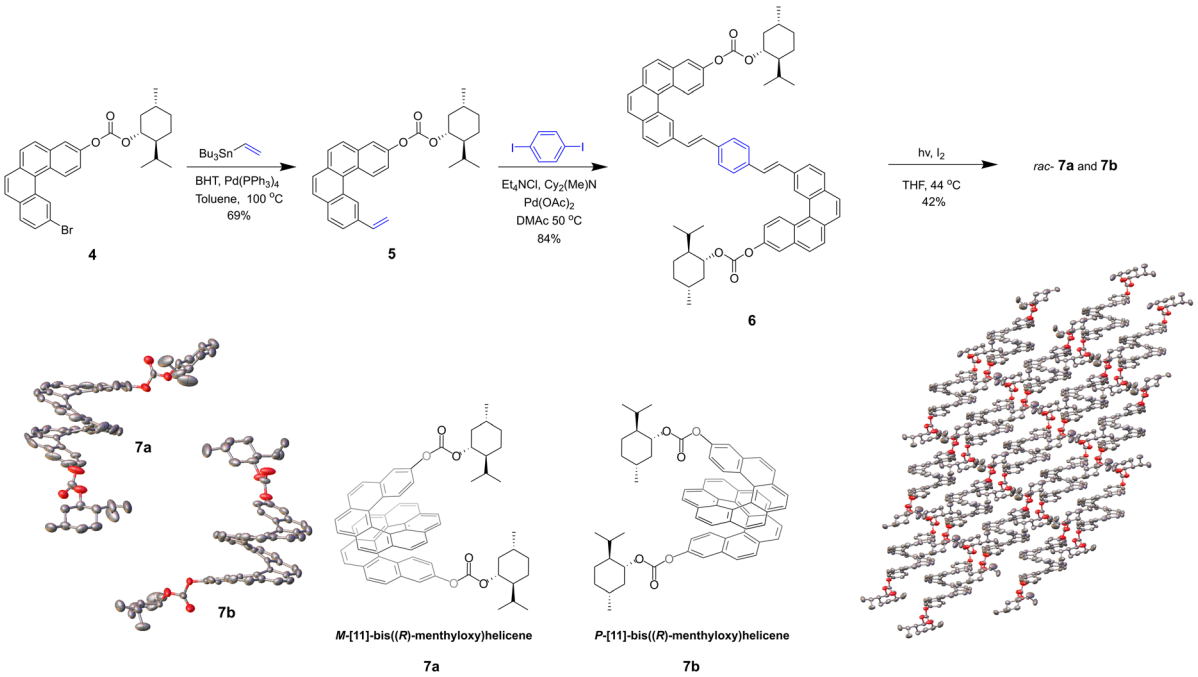

Scheme 2 Synthesis of *rac*-[11]bis(menthyloxycarbonato)helicene accompanied by crystal structure (left) and its packing (right). Racemic mixture is labeled from the standpoint of *P* and *M*-[11]-helicene, ignoring stereochemistry of the menthyloxycarbonato groups. Butylated hydroxytoluene is abbreviated as BHT.

ethylene glycol solution to lower the reaction temperature to sub-ambient conditions with the ability to precisely control the temperature of the reaction solvent *via* an external thermocouple.

Equilibrating the reaction temperature at ~14 °C, the photocyclization reaction yielded the helical product, with a final isolated yield of ~3% after a total reaction time of 144 hours in the photoreactor. In order to further investigate the impact of reaction temperature on the nature of the photocyclization reaction, additional small scale exploratory vial reactions were performed at ambient temperature between 20 °C and 25 °C. The findings from these experiments indicated that at ambient temperatures faster reaction rates were observed, with full consumption of starting material in 53 hours, with no noticeable increase in the magnitude of impurity resonances as observed *via* ^{1}H NMR. The vial scale reactions were scaled up to the 1 L photoreactor with the ethylene glycol chiller adjusted until the temperature of the reaction solvent was stabilized at 24 °C after the UV light source reached full power. As observed in the vial scale tests, the reaction appeared to proceed at an elevated rate compared to sub-ambient temperatures, however over-exposure to UV irradiation appeared to cause transformation of helicene product after the same 144 hours reaction period.

Thus, in order to balance the preferential formation of the kinetic helicene product while mitigating photo-driven product transformation arising from extended UV exposure, an intermediate reaction time of 91 hours was observed as the point of full conversion of the starting material at 24 °C. After a similar purification process to the previous large scale reaction, the final isolated yield of **7** was increased from ~3% to ~10%. Many unaccounted for aromatic resonances exist in the pre-work up material, as well as resonances in the 2–4 ppm region of the ^{1}H NMR, which have been previously associated with protons in cyclobutane derivatives arising from undesirable [2 + 2] cycloadditions.[26] This leads to our hypothesis that linear products [2 + 2] products, pseudo-helical, and various other products of the aforementioned species all compete with the formation of helical product.

Based on the observed trend of increasing temperature affording improved reaction yields, a final trial at the 1 L scale was performed at an increased reaction temperature of 44 °C using a hot water supply, measured to be 31 °C. The total residence time in the photoreactor in this trial was 66 hours with an isolated yield of 42%. A summary the relationship between isolated yield and temperature can be found in Fig. 2. The ^{1}H NMR spectra of pre-worked up material was less complicated, with many aromatic resonances and resonances in the cyclobutane region previously observed in the sub-ambient and ambient temperature trials were no longer observed in the elevated temperature experiment. We postulate that the increase in temperature assists in the photoinduced *trans* to *cis* isomerization of **6** allowing for a greater probability of bond formation between the carbons adjacent to the double bond and subsequent oxidation of the dihydrophenanthrene-like intermediate to form the fused-ring backbone. In turn, this reduces the probability of intermolecular side reactions, such as the [2 + 2] cycloaddition, as there is less of a chance for reaction-inducing collisions before annulation occurs.

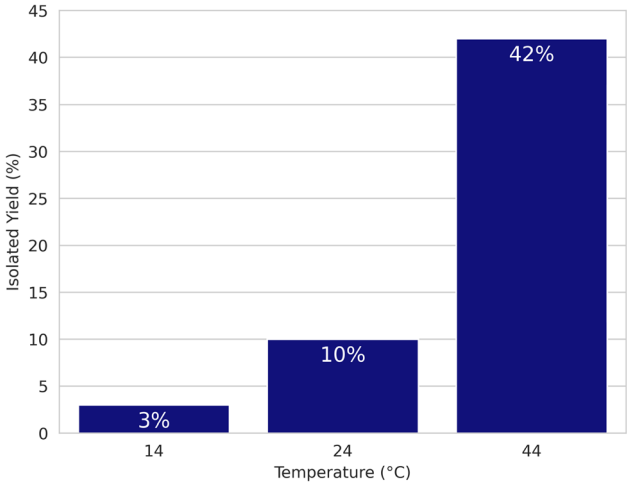

Fig. 2 Temperature influence on isolated yield of **7**. Reaction termination was determined based on full consumption of starting material *via* ^{1}H NMR. The time to achieve conversion was determined to be 144, 91, and 66 hours (Left to Right).

In our study, the isolated yields of **7** were noticeably lower than the similar [4] + [1] + [4] system shown by Martin and Baes in 1975, who reported an 84% isolated yield of [11]-carbohelicene upon photocyclization. It is evident that the photocyclization of **6** is improved by providing sufficient activation energy to increase the rate of *trans* to *cis* isomerization which is required before C–C bond formation can occur between the adjacent rings to form the helicene backbone. Avoiding the need to undergo *trans* to *cis* isomerization could indicate that formulating a synthetic route to the *Z*-bisarylethenes, as was done in Baes and Martin's work through a Wittig reaction, over the *E*-bisarylethenes typically produced *via* organometallic couplings, provides a predisposition to form helicene over other side products by reducing the energetic barrier required for annulation to the helical product. It should be noted that the Wittig route to helicene precursors is most useful for non-functional (carbohelicene) products as precursors containing more diverse chemical functionality (*i.e.* menthyl carbonate groups) would complicate desired *Z*-alkene formation.

Though direct studies on the effect of molecular orbital populations on the annulation products of bis(aryl)ethenes are not widely reported in the literature, there are still indications that manipulating the electronic structure of bis(aryl)ethenes could have significant impacts on the outcome of photocyclization of studied substrates. Matsuda *et al.* found that the introduction of electron-withdrawing groups to the C-5 and C-10 positions of [5]-helicene significantly suppressed the undesired over-annulation of the [5]-helicene by removing orbital degeneracy of lower UMOs (unoccupied molecular orbitals), stabilizing the C_2-antisymmetric UMO, and making it such that the only transition is not suitable for conrotary cyclization, reducing the amount of over-annulated product in their cyano-substituted [5]-helicene.[27] A similar affect may be occurring with the cyclization of **6**, where the menthyl-carbonate groups could be stabilizing the symmetric UMO configuration such that the helical product is less favored for conrotary cyclization compared to other side products. Further computational modeling as well as a systematic study of substituent effects on the photocyclization product distribution could provide deeper insight into the specifics of the reaction and begin to establish a design framework for optimization of synthesizing specific structural isomers.

In alignment with our interest in obtaining enantiopure helicenes for future applications, diastereomeric separation of **7** has been achieved on an analytical scale LC-MS using a Waters XBridge BEH phenyl OBD column (2.1 × 50 mm with a 1.7 μm particle size) using 99.5 : 0.5 MeCN : toluene as mobile phase eluting at 0.050 mL min^{-1}. The transfer of analytical scale conditions to preparative scale LC-MS using a number of different column compositions and mobile phases is currently being explored. Fortuitously, an interesting phenomenon was observed when recrystallizing a small sample (5 mg) of **7** using acetonitrile during small-scale purification development. Upon isolating the recrystallized solids, it was found that the crystals were diastereomerically enriched when characterized using ^{1}H NMR and by CD spectroscopy shown in Fig. 3. This behavior could be used to assist in the synthesis of diastereomerically pure **7** at scale in the future by using diastereomerically pure crystals to seed growth at a large scale, potentially avoiding the use of preparative LC. The synthesis of this functionalized [11]-helicene enables the validation of spring-force models, the development of elastomeric materials for strain sensing materials, and postures the team to develop even longer order helicenes.

All synthesized materials were characterized *via* ^{1}H and ^{13}C NMR spectroscopy as well as single-crystal X-ray diffractometry, except for **6** in which suitable crystals could not be grown. High-resolution mass spectroscopy for all synthesized compounds determined using a Waters Corporation Xevo G3 QToF with electrospray ionization in positive mode (ES+) with solutions of concentrations ~1 ng mL^{-1}. A Bruker Ascend™ 400 MHz NMR spectrometer was used to collect ^{1}H and ^{13}C NMR spectra for all materials. X-ray intensity data was collected on a Rigaku XtaLAB Synergy-S, PhotonJet-i with a CCD detector using Cu Kα radiation ($\lambda = 1.5406$ Å). Images were interpreted and integrated with CrysAlisPRO and structures were solved using Olex2 with the ShelXT solution program and further refinement using ShelXL.[28] Non-hydrogen atoms were refined anisotropically.

CCDC 2428292–2428297 contain the supplementary crystallographic data for this paper. These data are provided free of charge by the Cambridge Crystallographic Data Centre.

Single crystal X-ray diffractometry

Single crystals of **1** were grown *via* the bulk recrystallization in methanol to afford colorless, needle-like crystals. Colorless, plate-like crystals of **2** were formed *via* bulk recrystallization in heptane. Colorless, plate-like crystals of **3** were formed *via* bulk recrystallization in acetonitrile. Small, colorless crystals of **4** were formed *via* bulk recrystallization in acetonitrile.

Crystal structure determination of compound 4. Crystal data for $C_{58}H_{58}BrO_6$ (1010.86 g mol^{-1}): monoclinic, space group $P2_1$,

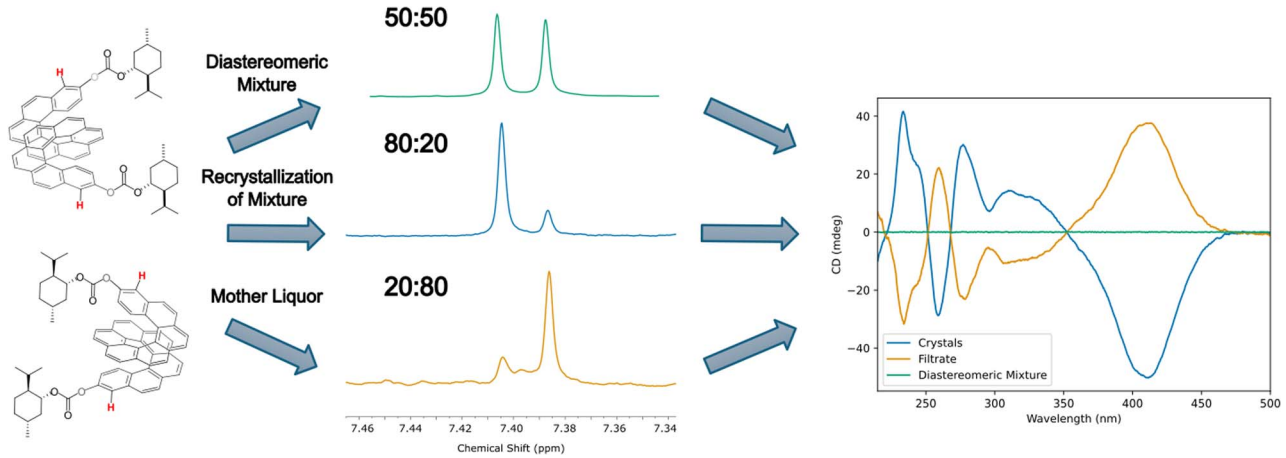

Fig. 3 CD and NMR (protons 4 and 4′) of diastereomerically-enriched **7**. Full ^{1}H NMR spectrum of **7** available in ESI.†

$a = 9.26620(10)$ Å, $b = 8.5188(2)$ Å, $c = 31.2770(4)$ Å, $\alpha = 90°$, $\beta = 93.4810(10)°$, $\gamma = 90°$, $V = 2464.35(7)$ Å^3, $Z = 2$, $\rho_{calc} = 1.362$ g cm^{-3}, 18 195 reflections measured ($8.496° \leq 2\phi \leq 153.586°$), 7620 independent ($R_{int} = 0.0328$, $R_{sigma} = 0.0388$). Final $R_1 = 0.0407$ [$I > = 2\sigma(I)$] and w$R_2 = 0.1102$ [all data].

Single crystals of **5** were grown *via* the bulk recrystallization in hexanes to afford colorless, needle-like crystals. Crystals of **6** could not be grown sufficiently for single crystal XRD. Crystalline solids of **7** were collected *via* the bulk recrystallization in acetonitrile.

Crystal structure determination of compound 7. Crystal data for $C_{68}H_{62}O_6$ (975.17 g mol^{-1}): monoclinic, space group *I*2, $a = 24.4751(10)$ Å, $b = 14.97496(10)$ Å, $c = 30.6550(13)$ Å, $\alpha = 90°$, $\beta = 151.936(12)°$, $\gamma = 90°$, $V = 5285.7(10)$ Å^3, $Z = 4$, $\rho_{calc} = 1.225$ g cm^{-3}, 74 976 reflections measured ($3.668° \leq 2\phi \leq 154.756°$), 10 128 independent ($R_{int} = 0.0197$, $R_{sigma} = 0.0108$). Final $R_1 = 0.0774$ [$I > = 2\sigma(I)$] and w$R_2 = 0.2301$ [all data].

Crystallographic analysis of compounds **4** and **7** confirmed the anticipated synthetic outcomes, helicene over linear, as well bond lengths and torsion angles that are common in these helical structures. In the inner helix, the average C–C bond length of **4** at 1.45 Å *versus* all other bond lengths (outer helix, terminal aromatic rings), deviates from an ideal aromatic bond of 1.39 Å. The same can be said of **7** and is attributed to the non-planar, strained conformation of helicenes relative to planar linear structural isomers. The solved crystal structure and packing of **4** and **7** can be found in Schemes 1 and 2 respectively.

Crystallographic parameters of **1**, **2**, **3** and **5** can be found in the ESI† of this manuscript.

Experimental

Synthesis of 6-bromonaphthalen-2-yl (2-isopropyl-5-methylcyclohexyl) carbonate, 1

To a 1 L three – necked round bottom, 6-bromo-2-naphthol (14.423 g, 64.650 mmol), triethylamine (20.0 mL, 133 mmol), and 100 mL of toluene were charged. Reaction mixture was stirred until homogeneity. (1*R*)-(+)-Menthyl chloroformate (14.0 mL, 65.3 mmol) in 100 mL of toluene was added over the course of an hour *via* an addition funnel. Colorless precipitate formed upon addition of all reagents. Reaction ran at room temperature for 18 hours. Volatiles were removed on rotary evaporator and reaction mixture was re-dissolved in 500 mL of toluene. Reaction solution was washed with 3 × 250 mL 2 M HCl and 3 × 300 mL of deionized water. Organic layer collected and dried over Na_2SO_4. Volatiles removed on rotatory evaporator to afford orange solid. Solids recrystallized from 450 mL of methanol to afford off colorless crystalline solid (23.744 g, 91% yield). ^{1}H NMR (δ, $CDCl_3$, 400 MHz): 0.857 (d, 3H), 0.954 (dd, 7H), 1.093 (m, 1H), 1.170 (q, 1H), 1.505 (m, 1H), 4.655 (q, 1H), 7.340 (dd, 1H), 7.553 (dd, 1H), 7.635 (d, 1H), 7.672 (d, 1H), 7.752 (d, 1H), 7.995 (d, 1H). ^{13}C NMR (δ, $CDCl_3$, 101 MHz): 16.396, 20.765, 22.004, 23.394, 26.275, 31.457, 34.057, 40.662, 47.055, 79.788, 118.081, 119.678, 121.822, 128.546, 129.324, 129.808, 130.048, 132.139, 132.414, 149.091, 153.263. ES+ calcd for $C_{21}H_{25}BrNaO_3$: *m*/*z* 427.0884 observed: *m*/*z* 427.0879.

Synthesis of 2-isopropyl-5-methyl-cyclohexyl (6-vinylnaphthalen-2-yl) carbonate, 2

To a 200 mL Schlenk flask, **1** (50.022 g, 123.41 mmol), tributyl(vinyl)tin (39.62 mL, 135.6 mmol), butylated hydroxytoluene (few crystals), tetrakis(triphenylphosphine) palladium(0) (2.837 g, 2.455 mmol), and 250 mL of toluene were charged in inert argon glovebox. Reaction was transferred to Schlenk line and heated at 100 °C for 18 hours. Reaction mixture was concentrated *via* rotary evaporator to afford grey, greasy solid. Grey solid was deposited on silica and flash chromatography (1% EtOAc : hexanes on 10 wt% K_2CO_3 : silica) performed to afford puffy colorless solid. Recrystallization from heptane afforded colorless crystalline solid (33.431 g, 77% yield). ^{1}H NMR (δ, $CDCl_3$, 400 MHz): 0.860 (d, 3H), 0.913 (d, 1H), 0.956 (d, 6H), 1.097 (m, 1H), 1.171 (q, 1H), 1.522 (m, 2H), 1.718 (m, 2H), 2.080 (m, 1H), 2.202 (m, 1H), 4.656 (m, 1H), 5.340 (d, 1H), 5.866 (d, 1H), 6.865 (dd, 1H), 7.301 (dd, 1H), 7.621 (d, 1H), 7.649 (dd, 1H), 7.757 (m, 2H), 7.815 (d, 1H). ^{13}C NMR (δ, $CDCl_3$, 101 MHz): 16.389, 20.770, 22.004, 23.392, 26.259, 31.457,

34.075, 40.676, 47.061, 79.635, 114.385, 117.907, 121.021, 124.028, 126.122, 127.952, 129.526, 131.542, 133.383, 135.021, 136.696, 148.919, 153.410. ES+ calcd for $C_{23}H_{28}NaO_3$: *m*/*z* 375.1936 observed: *m*/*z* 375.1930.

Synthesis of (*E*)-6-(4-bromostyryl)-naphthalen-2-yl (2-isopropyl-5-methyl-cyclohexyl) carbonate 3

To a 200 mL Schlenk flask, **2** (13.089 g, 37.134 mmol), *p*-bromoiodobenzene (11.473 g, 40.554 mmol), tetraethylammonium chloride (6.141 g, 36.88 mmol), *N*,*N*-dicyclohexylmethylamine (11.8 mL, 55.3 mmol), palladium(II) acetate (84.5 mg, 0.369 mmol), and 105 mL of DMAc were charged in an inert argon glove-box. Reaction flask was transferred to inert argon Schlenk line and heated at 50 °C for 40 hours. DMAc was then distilled *via* short path distillation apparatus at a reduced pressure of 1 mTorr and nitrogen at the receiving flask. Deionized water was then added to the resulting orange solids along with dichloromethane until all solids were dissolved. The organic layer was washed with deionized water 3*x* and a saturated brine solution 1*x*. The organic layer was collected and dried over Na_2SO_4 and volatiles were removed on the rotatory evaporator. The resulting yellow-brown solids were dissolved in hot MeCN, treated with activated carbon, filtered off remaining undissolved solids, and recrystallized from acetonitrile to afford colorless crystalline solid (14.406 g, 77% yield). ^{1}H NMR (δ, $CDCl_3$, 400 MHz): 0.866 (d, 3H), 0.9191 (d, 1H), 0.961 (d, 6H), 1.110 (m, 1H), 1.178 (q, 1H), 1.529 (m, 2H), 1.725 (m, 2H), 2.085 (m, 1H), 2.207 (d, 1H), 4.663 (m, 1H) ^{13}C NMR (δ, $CDCl_3$, 101 MHz) 0.02 16.39, 20.77, 22.01, 23.40, 26.26, 31.46, 34.08, 40.68, 47.06, 76.71, 77.03, 77.23, 77.35, 79.64, 114.39, 117.91, 121.02, 124.03, 126.13, 127.96, 129.53, 131.54, 133.39, 135.02, 136.70, 148.92, 153.41. ESI+ calcd for $C_{29}H_{31}BrNaO_3$: *m*/*z* 529.1354 observed: *m*/*z* 529.1349.

Synthesis of 11-bromo-benzophenanthren-3 yl (2-isopropyl-5-methyl-cyclohexyl) carbonate, 4

To a 1 L photoreaction vessel equipped with mercury arc lamp, 600 mL of THF along with 28 mL of propylene oxide was added and sparged under argon for 10 minutes. To a 50 mL glass/Teflon syringe, **3** (2.031 g, 4.035 mmol), iodine (1.523 g, 6.010 mmol), and THF (40 mL) were charged. Upon activation of the mercury arc lamp, the reaction solution was added at a rate of 3 mL per hour. With a 50/50 ethylene glycol/water recirculating chiller, reaction vessel temperature equilibrated to 14 °C. Upon full addition of reagents, reaction was left to run for an additional 2 hours. The reaction mixture was then transferred to a 2 L Erlenmeyer flask and an aqueous solution of ascorbic acid (12 mmol in 100 mL of water) was added and stirred until solution was very light yellow. Solution was then concentrated *via* rotatory evaporator to remove organic volatiles. Resulting orange oil was dissolved in 500 mL of DCM and washed with 300 mL of water 3×. Organic layer was collected, dried over Na_2SO_4, and organic volatiles removed on rotatory evaporator. Remaining solids were recrystallized from MeCN to afford colorless crystalline solid (1.691 g, 84%). ^{1}H NMR (δ, $CDCl_3$, 400 MHz): 0.890 (d, 3H), 0.940 (d, 1H), 0.980 (m, 6H), 1.120 (q, 1H), 1.219 (q, 1H), 1.545 (m, 2H), 1.743 (m, 2H), 2.124 (m, 1H), 2.250 (m, 1H), 4.710 (m, 1H), 7.580 (dd, 1H), 7.715 (dd, 1H), 7.861 (m, 6H), 9.041 (d, 1H), 9.219 (s, 1H). ^{13}C NMR (δ, $CDCl_3$, 101 MHz) 16.41 20.78, 22.01, 23.39, 26.28, 31.46, 34.06, 40.68, 47.07, 77.22, 79.79, 119.03, 120.60, 120.73, 126.22, 127.04, 127.22, 127.59, 127.66, 127.93, 128.83, 129.20, 129.97, 130.04, 131.19, 131.29, 131.97, 134.28, 148.93, 153.40. ES+ calcd for $C_{29}H_{29}BrNaO_3$: *m*/*z* 527.1197 observed: *m*/*z* 527.1192.

Synthesis of 2-isopropyl-5-methyl cyclohexyl (11-vinylbenzo[*c*] phenanthren-3-yl) carbonate, 5

To a 10 mL Schlenk flask, **4** (504 mg, 1.00 mmol), tributyl(vinyl) tin (0.320 mL, 1.10 mmol), butylated hydroxytoluene (few crystals), tetrakis(triphenylphosphine)palladium(0) (24.0 mg, 0.021 mmol), and 2 mL of toluene were charged in an inert argon glovebox. Reaction flask was *trans*-ferred to inert argon Schlenk line and heated at 100 °C for 24 hours. Toluene was then concentrated off *via* rotary evaporator and dried on high vacuum overnight affording a gummy gray solid. Solid was dry deposited onto silica and flash chromatography performed (5% EtOAc : hexanes) to afford colorless solid. Solids recrystallized from hexanes to afford colorless crystalline solid (310 mg, 69% yield). ^{1}H NMR (δ, $CDCl_3$, 400 MHz): 0.820 (d, 3H), 0.902 (t, 3H), 1.052 (m, 1H), 1.134 (q, 1H), 1.468 (m, 2H), 1.659 (m, 2H), 2.047 (m, 1H), 2.171 (m, 1H), 4.631 (td, 1H), 5.332 (d, 1H), 5.874 (d, 1H), 6.919 (dd, 1H), 7.459 (dd, 1H), 7.695 (dd, 2H), 7.759 (m, 4H), 7.883 (d, 1H), 8.911 (s, 1H), 9.024 (d, 1H). ^{13}C NMR (δ, 101 MHz, $CDCl_3$): 14.16. 16.44, 20.81, 22.04, 23.43, 26.31, 31.50, 31.62, 34.10, 40.73, 47.11, 76.73, 77.04, 77.25, 77.36, 79.73, 79.77, 114.53, 118.93, 120.14, 123.28, 126.54, 126.84, 127.04, 127.11, 127.22, 127.38, 127.83, 128.27, 128.86, 129.29, 130.31, 131.12, 133.25, 134.31, 135.58, 137.32, 148.81, 153.49. ES+ calcd for $C_{31}H_{32}NaO_3$: *m*/*z* 475.2249 observed: *m*/*z* 475.2243.

Synthesis of 1,4-phenylenebis(ethene-2,1-diyl) bis(benzo[*c*] phenanthrene-11,3-diyl)(bis-2-isopropyl-5-methylcyclohexyl) bis(carbonate), 6

To a 25 mL Schlenk flask, **5** (1.285 g, 2.841 mmol), 1,4-diiodobenzene (458 mg, 1.38 mmol), tetraethylammonium chloride (229 mg, 1.38 mmol), *N*,*N*-dicyclohexylmethylamine (0.750 mL, 3.45 mmol), palladium (II) acetate (3.3 mg, 0.014 mmol), and 14 mL of DMAc were charged in an inert argon glovebox. The reaction vessel was then transferred to an inert argon Schlenk line and heated at 90 °C for 20 hours. DMAc was then distilled off under high vacuum. Residual yellow solids were washed with Et_2O, filtrate was discarded, and then solids dissolved in DCM and washed with equivalent amount of aqueous 1 M $NaHCO_3$ 3×. Organic layer collected and dried over Na_2SO_4, filtered, concentrated *via* rotary evaporator, and dried on high vacuum. Resulting yellow solids were washed with copious amount of MeOH and water to afford powdery yellow solid (1.138 g, 84% yield). ^{1}H NMR (δ, $CDCl_3$, 400 MHz): 0.913 (d, 6H), 0.993 (t, 12H), 1.139 (m, 2H), 1.228 (q, 2H), 1.549 (m, 4H), 1.751 (m, 4H), 2.145 (m, 2H), 2.265 (m, 2H), 4.725 (m, 2H), 7.400 (dd, 4H), 7.615 (dd, 2H), 7.66 (s, 4H), 7.810 (d, 2H), 7.935 (d, 2H), 8.03 (d, 2H), 9.11 (s, 2H), 9.18 (d, 2H). ^{13}C NMR (δ, 101 MHz, $CDCl_3$):

16.46, 20.82, 22.05, 23.44, 26.33, 31.51, 34.11, 40.74, 47.12, 76.72, 77.04, 77.24, 77.36, 79.79, 118.95, 120.25, 123.33, 126.84, 127.08, 127.14, 127.16, 127.24, 127.34, 127.86, 128.31, 128.94, 129.04, 129.10, 129.34, 130.52, 131.21, 133.16, 134.34, 135.45, 136.85, 148.84, 153.53. ES+ calcd for $C_{68}H_{66}NaO_6$: *m*/*z* 1001.4757 observed: *m*/*z* 1001.4750.

Synthesis of 3,3′-(bis-2-isopropyl-5-methylcyclohexyl) bis(carbonate) [11] helicene, 7

To a 1 L photoreaction vessel equipped with mercury arc lamp, 530 mL of THF, **6** (368 mg, 0.376 mmol), and iodine (386 mg, 1.53 mmol) was added and sparged under argon for 10 minutes. Hot water was used to chill photoreaction vessel and temperature of mixture maintained at 44 °C. Reaction vessel was irradiated with UV-light from a mercury arc lamp for 66 hours. Flash chromatography was performed (5 : 95 dioxane : heptane) to afford powdery yellow solid (154 mg, 42% yield). ^{1}H NMR (δ, $CDCl_3$, 400 MHz): 0.880 (q, 8H), 0.972 (dd, 14H), 1.138 (m, 5H), 1.549 (m, 4H), 1.733 (m, 4H), 2.044 (m, 2H), 2.178 (m, 2H), 4.625 (sep, 2H), 6.001 (dt, 2H), 6.681 (d, 2H), 7.114 (m, 4H), 7.282 (m, 14H), 7.394 (d, 2H). ^{13}C NMR (δ, 101 MHz, CD_2Cl_2): 17.48, 17.52, 21.85, 23.10, 24.70, 24.72, 27.59, 27.64, 31.01, 32.78, 35.42, 42.02, 48.49, 48.54, 80.41, 118.06, 118.11, 118.15, 123.98, 125.62, 125.94, 126.57, 126.77, 126.79, 127.26, 127.30, 127.40, 127.49, 127.67, 127.69, 127.78, 127.83, 127.89, 128.42, 131.25, 131.86, 132.82, 133.01, 133.59, 148.87, 154.49, 154.55. ES+ calcd for $C_{68}H_{62}NaO_6$: *m*/*z* 997.4444 observed: *m*/*z* 997.4443.

Data availability

The data underlying this study are available in the published article and its ESI.† FAIR data is available as ESI for publication and includes the primary NMR FID files for compounds: **1–7**. Crystallographic data for **1–5** and **7** has been deposited at the CCDC under 2428292–2428297 and can be obtained from **https://www.ccdc.cam.ac.uk/**.

Conflicts of interest

The author(s) declare no competing interests.

Acknowledgements

We acknowledge and are grateful for the support of the Air Force Office of Scientific Research for funding this effort (24RX-COR016), Contract Numbers FA8650-21 F-5237-0001 and FA8650-21-F-5238-0002. We extend our thanks to the SOCHE (Strategic Ohio Council for Higher Education) for providing student support that contributed to this work. We also deeply appreciate the guidance provided by Professor Stephen L. Buchwald on synthetic methodology, which were crucial in shaping our synthetic strategy.

References

1 Y. Shen and C.-F. H. Chen, Synthesis and Applications, *Chem. Rev.*, 2012, **112**, 1463–1535.
2 M. Gingras, One hundred years of helicene chemistry. Part 1: non-stereoselective syntheses of carbohelicenes, *Chem. Soc. Rev.*, 2013, **42**, 968–1006.
3 C. Nuckolls, T. J. Katz and L. Castellanos, Aggregation of Conjugated Helical Molecules, *J. Am. Chem. Soc.*, 1996, **118**, 3767–3768.
4 A. J. Lovinger, C. Nuckolls and T. J. Katz, Structure and Morphology of Helicene Fibers, *J. Am. Chem. Soc.*, 1998, **120**, 264–268.
5 T. R. Kelly, Progress toward a Rationally Designed Molecular Motor, *Acc. Chem. Res.*, 2001, **34**, 514–522.
6 A. P. Davis, Tilting at Windmills? The Second Law Survives, *Angew. Chem., Int. Ed.*, 1998, **37**, 909–910.
7 A. A. Frimer, J. D. Kinder, W. J. Youngs and M. A. B. Meador, Reinvestigation of the Photocyclization of 1,4-Phenylenebis [phenylmaleic anhydride]: Preparation and Structure of [5] Helicene 5,6:9,10-Dianhydride, *J. Org. Chem.*, 1995, **60**, 1658–1664.
8 Z. Y. Wang and J. E. Douglas, New Route to the Introduction of Axial and Helical Chiral Units into Poly(arylene ether)s, *Macromolecules*, 1997, **30**, 8091–8093.
9 T. T. Serafini, P. Delvigs and G. R. Lightsey, Thermally stable polyimides from solutions of monomeric reactants, *J. Appl. Polym. Sci.*, 1972, **16**, 905–915.
10 H. Kitajima, K. Ito, Y. Aoki and T. N. Katsuki, N,N,N-Tetraalkyl-2,2-dihydroxy-1,1-binaphthyl-3,3-dicarboxamides, Novel Chiral Auxiliaries for Asymmetric Simmons–Smith Cyclopropanation of Allylic Alcohols and for Asymmetric Diethylzinc Addition to Aldehydes, *Bull. Chem. Soc. Jpn.*, 2006, **70**, 207–217.
11 D. Nakano and M. Yamaguchi, Enantioselective hydrogenation of itaconate using rhodium bihelicenol phosphite complex. Matched/mismatched phenomena between helical and axial chirality, *Tetrahedron Lett.*, 2003, **44**, 4969–4971.
12 M. T. Reetz and S. Sostmann, Kinetic resolution in Pd-catalyzed allylic substitution using the helical PHelix ligand, *J. Organomet. Chem.*, 2000, **603**, 105–109.
13 X. Liu, X. Cui, X. Zhang, J.-P. Wu and C. Shen, A DFT study on spring property of helicenes, *Theor. Chem. Acc.*, 2024, **143**, 17.
14 J. Barroso, J. L. Cabellos, S. Pan, F. Murillo, X. Zarate, M. A. Fernandez-Herrera and G. Merino, Revisiting the racemization mechanism of helicenes, *Chem. Commun.*, 2018, **54**, 188–191.
15 P. Šesták, J. Wu, J. He, J. Pokluda and Z. Zhang, Extraordinary deformation capacity of smallest carbohelicene springs, *Phys. Chem. Chem. Phys.*, 2015, **17**, 18684–18690.
16 F. B. Mallory, C. S. Wood and J. T. Gordon, Photochemistry of Stilbenes. III. Some As-pects of the Mechanism of Photocyclization to Phenanthrenes, *J. Am. Chem. Soc.*, 1964, **86**, 3094–3102.
17 L. Liu, B. Yang, T. J. Katz and M. K. Poindexter, Improved methodology for photocyclization reactions, *J. Org. Chem.*, 1991, **56**, 3769–3775.
18 F. Teplý, I. G. Stará, I. Starý, A. Kollárovič, D. Šaman, L. Rulìšek and P. Fiedler, Synthesis of [5]-[6]-and [7]

Helicene *via* Ni(0)- or Co(I)-Catalyzed Isomerization of Aromatic cis,cis-Dienetriynes, *J. Am. Chem. Soc.*, 2002, **124**, 9175–9180.

19 P. Sehnal, I. G. Stará, D. Šaman, M. Tichý, J. Mìšek, J. Cvačka, L. Rulìšek, J. Chocholousová, J. Vacek, G. Goryl, M. Szymonski, I. Cìsarová and I. Starý, An organometallic route to long helicenes, *Proc. Natl. Acad. Sci. U. S. A.*, 2009, **106**, 13169–13174.

20 K. Mori, T. Murase and M. Fujita, One-Step Synthesis of [16] Helicene, *Angew. Chem., Int. Ed.*, 2015, **54**, 6847–6851.

21 G. P. Moss, P. A. S. Smith and D. Tavernier, Glossary of class names of organic compounds and reactivity intermediates based on structure (IUPAC Recommendations 1995), *Pure Appl. Chem.*, 1995, **67**, 1307–1375.

22 W. H. Laarhoven and W. J. C. Prinsen, *Carbohelicenes and Heterohelicenes. Stereochemistry*, Berlin, Heidelberg, 1984, pp. 63–130.

23 J. Seylar, D. Stasiouk, D. L. Simone, V. Varshney, J. E. Heckler and R. McKenzie, Breaking the bottleneck: stilbene as a model compound for optimizing 6π e photocy-clization efficiency, *RSC Adv.*, 2021, **11**, 6504–6508.

24 V. Farina, V. Krishnamurthy and W. J. Scott, *Organic Reactions*, John Wiley & Sons, Ltd, 2004, Ch. 1, pp. 1–652.

25 C. Gürtler and S. L. Buchwald, A Phosphane-Free Catalyst System for the Heck Aryla- tion of Disubstituted Alkenes: Application to the Synthesis of Trisubstituted Olefins, *Chem.–Eur. J.*, 1999, **5**, 3107–3112.

26 H. Amjaour, Z. Wang, M. Mabin, J. Puttkammer, S. Busch and Q. R. Chu, Scalable preparation and property investigation of a cis-cyclobutane-1,2-dicarboxylic acid from-trans-cinnamic acid, 2019 -trans-cinnamic acid, *Chem. Commun.*, 2019, **55**, 214–217.

27 N. Ito, T. Hirose and K. Matsuda, Facile Photochemical Synthesis of 5,10-Disubstituted [5]Helicenes by Removing Molecular Orbital Degeneracy, *Org. Lett.*, 2014, **16**, 2502–2505.

28 O. V. Dolomanov, L. J. Bourhis, R. J. Gildea, J. A. K. Howard and H. Puschmann, OLEX2: a complete structure solution, refinement and analysis program, *J. Appl. Crystallogr.*, 2009, **42**, 339–341.